

# Condensation induced by coupled transport processes

Gabriele Gotti,<sup>1,2</sup> Stefano Iubini,<sup>2,3,\*</sup> and Paolo Politi<sup>2,3,†</sup>

<sup>1</sup>*Dipartimento di Fisica e Astronomia, Università di Firenze,  
via G. Sansone 1 I-50019, Sesto Fiorentino, Italy*

<sup>2</sup>*Istituto dei Sistemi Complessi, Consiglio Nazionale delle Ricerche,  
via Madonna del Piano 10, I-50019 Sesto Fiorentino, Italy*

<sup>3</sup>*Istituto Nazionale di Fisica Nucleare, Sezione di Firenze,  
via G. Sansone 1 I-50019, Sesto Fiorentino, Italy*

(Dated: November 14, 2022)

Several lattice models display a condensation transition in real space when the density of a suitable order parameter exceeds a critical value. We consider one of such models with two conservation laws, in a one-dimensional open setup where the system is attached to two external reservoirs. Both reservoirs impose subcritical boundary conditions at the chain ends. When such boundary conditions are equal, the system is in equilibrium below the condensation threshold and no condensate can appear. Instead, when the system is kept out of equilibrium, localization may arise in an internal portion of the lattice. We discuss the origin of this phenomenon, the relevance of the number of conservation laws, and the effect of the pinning of the condensate on the dynamics of the out-of-equilibrium state.

## I. INTRODUCTION

Real-space condensation phenomena represent a vast class of processes that appear in many domains of physics. Typical examples from the classical realm are the behavior of traffic flows, the dynamics of shaken granular media, the aggregation and fragmentation processes, the localization in real-world networks, phase transitions in stochastic mass transport models, nonlinear propagation in weakly dissipative systems [1–12]. All these systems may display a phase transition from a homogeneous phase to a localized one when varying a suitable control parameter, which is often the density of a conserved quantity of the system: above a critical density a finite fraction of the conserved quantity is localized on a single lattice site, while the remaining amount is delocalized over the rest of the system [13–17]. In the absence of intrinsic dishomogeneities such as spatial disorder [18, 19], each lattice site is equally eligible to host the condensate.

So far, the condensation transition has been studied in details in a large variety of equilibrium models and in translationally invariant, bulk-driven diffusive models [20]. In the latter case, the nonequilibrium condition is ascribable to the presence of a bias in the microscopic dynamics which breaks detailed balance in a system with periodic boundary conditions. Hence macroscopic circulating currents are steadily induced. In some cases, e.g. in the Zero-Range Processes (ZRP) [6], the bias breaks detailed balance but the nonequilibrium steady state equals the equilibrium state of the same model when hopping is made symmetric.

In this paper we intend to analyze a boundary-driven model where translational invariance is broken and which

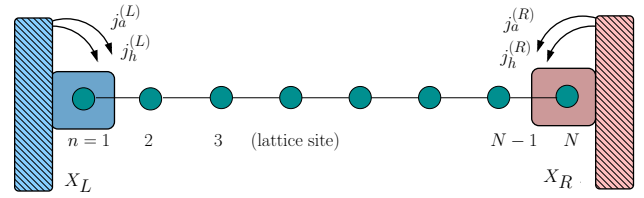


FIG. 1. The setup: a one-dimensional lattice with  $N$  sites interacts with two external reservoirs at its boundaries.  $X_L$  and  $X_R$  are the thermodynamic parameters imposed at the left and right side, respectively. Each reservoir exchanges with the system two distinct quantities (mass  $a$  and energy  $h$ , see text), which are transported through the chain. The corresponding fluxes from the reservoirs to the system are denoted by  $j_{a,h}^{(L,R)}$ , see Sec. II. In our case  $X_L$  and  $X_R$  are such that left currents are negative and right currents are positive. In a steady state there is a perfect balance between them,  $j^{(L)} + j^{(R)} = 0$ .

is genuinely off-equilibrium because the system is in contact with two different thermal reservoirs at its ends. In this setup bulk dynamics is assumed to be reversible, local equilibrium may appear, and conservation laws are relevant for the dynamics. Condensation in the context of such an open, out-of-equilibrium system has been much less explored. Asymmetric boundary conditions have been studied for ZRP, i.e. in models with a single conservation law, but in this case condensation appears only if a boundary condition is overcritical [21], i.e. if a reservoir imposes a localized equilibrium state.

In this paper we provide evidence that a new condensation mechanism may arise in out-of-equilibrium conditions but this occurs only if the system has two conservation laws. More precisely, we focus on a setup in which a one-dimensional lattice chain with local interactions and two conserved quantities is in contact with external reservoirs imposing thermodynamic parameters  $X_L$  and  $X_R$

\* stefano.iubini@cnr.it

† paolo.politi@cnr.it

at its left and right boundaries, respectively, see Fig. 1. Importantly, we consider the case in which both  $X_L$  and  $X_R$  are in the homogeneous, delocalized phase. With this constraint, in equilibrium conditions ( $X_L = X_R$ ) condensation is always forbidden. On the other hand, we find that when  $X_L \neq X_R$  localization may arise in the bulk of the system.

As we will see, the existence of two conservation laws implies a coupled transport process which is essential to induce condensation. We will also show that the properties of the asymptotic, out-of-equilibrium state depend on the possibility that the condensate may diffuse or not in space. If diffusion is allowed, the system attains a nonequilibrium steady state; if the condensate is pinned, it does not stop growing and stationarity is lost.

The paper is organized as follows. In Sec. II we introduce the model and discuss its equilibrium properties. In Sec. III we present the phenomenon of condensation occurring in a coupled-transport setup and we separately analyze the case of pinned and unpinned dynamics. Finally, in Sec. IV we provide a discussion of the main results and in Sec. V we outline the major open problems and perspectives.

## II. THE MODEL AND ITS EQUILIBRIUM PROPERTIES

The model we are going to describe can be derived from the Discrete Nonlinear Schrödinger (DNLS) equation [22], which is ubiquitous in nonlinear physics with applications in optics, cold-atoms physics and micro-magnetic systems. In its standard form, the DNLS equation reads

$$i\dot{z}_n = -2|z_n|^2 z_n - z_{n+1} - z_{n-1} \quad (1)$$

where  $z_n$  are complex-valued amplitudes defined on a one-dimensional lattice with  $1 \leq n \leq N$ . This equation displays two exactly conserved quantities, namely the total energy

$$H = \sum_n |z_n|^4 + z_n^* z_{n+1} + z_n z_{n+1}^* \quad (2)$$

and the total norm of the wavefunction

$$A = \sum_n |z_n|^2, \quad (3)$$

also called total ‘‘mass’’ [23]. For this reason, the model displays coupled transport when it is steadily maintained out of equilibrium [24, 25]. Above a certain critical energy density which depends quadratically on the mass density, the DNLS model also exhibits a condensation transition with a very rich phenomenology that involves the excitation of *discrete breather* states [23, 26] and includes the creation of negative-temperature states [26], extremely slow thermalization [27], inequivalence of statistical ensembles [28], and ergodicity breaking [29]. Its

equilibrium picture has recently reached a systematic and accurate description within the so-called large deviation theory [28, 30]. This has been possible because near the transition the DNLS model simplifies, as the hopping energy ( $z_n^* z_{n+1} + c.c.$ ) in Eq. (2) becomes negligible with respect to the local energy  $|z_n|^4$  [28]. The resulting simplified model, which is the object of our study, can be therefore expressed in terms of the local masses  $c_n = |z_n|^2 \geq 0$  only. We refer to this model as C2C [17], see Fig. 2, because it displays condensation in the presence of two conserved quantities, the mass  $A$  and the energy  $H$ ,

$$A = \sum_{n=1}^N c_n, \quad (4)$$

$$H = \sum_{n=1}^N c_n^2. \quad (5)$$

The thermodynamic behavior of the C2C model in equilibrium is specified by the values of the mass density  $a = H/N$  and of the energy density  $h = H/N$ . Therefore one can profitably represent all equilibrium states in the plane  $(a, h)$ , see Fig 3. In order to identify the main features of the equilibrium diagram, it is useful to evaluate the variance of the mass distribution,

$$\sigma^2 = \overline{c^2} - \bar{c}^2 = h - a^2, \quad (6)$$

which shows that it must be  $h \geq a^2$ . For  $h = a^2$ ,  $c_n \equiv a$  and  $\sigma = 0$ . With increasing  $h$  (at fixed  $a$ ) the variance of the mass distribution increases until the standard variation of the (positive) mass equals its average value. This occurs at the critical line  $h = 2a^2$ , where the mass is distributed exponentially [23]. Above this line a condensation process occurs and in the thermodynamic limit a single site hosts the extra-energy  $(h - 2a^2)N$ .

A more detailed description of equilibrium states is obtained from the evaluation of the grand canonical partition function [31, 32] derived in App. A,

$$Z(\beta, \mu) = \left[ \int_0^{+\infty} dc e^{-\beta(c^2 - \mu c)} \right]^N, \quad (7)$$

where  $\beta$  and  $\mu$  are the inverse temperature and the chemical potential, respectively. Using the standard formulas  $a = \langle A \rangle / N$  and  $h = \langle H \rangle / N$ , where the symbol  $\langle \cdot \rangle$  denotes the average over the grand canonical distribution, we find the equations

$$a = \frac{\mu}{2} + \frac{1}{\sqrt{\pi\beta}} \frac{e^{-\beta\mu^2/4}}{1 + \operatorname{erf}\left(\frac{\sqrt{\beta}\mu}{2}\right)} \quad (8)$$

$$h = \frac{1}{2\beta} + \frac{1}{2}a\mu, \quad (9)$$

which allow to connect  $(a, h)$  to  $(\beta, \mu)$  and vice versa. The details of the calculation are reported in Appendix A. In particular it is found that the critical

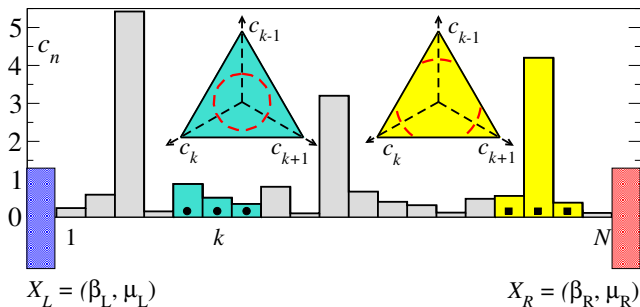


FIG. 2. Sketch of the C2C model with open boundary conditions: the two reservoirs interact at the boundaries of the chain and impose thermal parameters  $X_L = (\beta_L, \mu_L)$  and  $X_R = (\beta_R, \mu_R)$ . The bulk dynamics is realized by implementing the MMC algorithm (see text) on random triplets of consecutive sites. Conservation of energy and mass restricts the available states in the space  $(c_{k-1}, c_k, c_{k+1})$  either on a circle or on the union of three distinct arcs (red dashed lines).

parabola  $h = 2a^2$  corresponds to  $T \equiv 1/\beta = +\infty$  and  $\beta\mu = -1/a$ , while the parabola  $h = a^2$  corresponds to  $T = 0$  and  $\mu = 2a$ . States below the  $T = 0$  line are forbidden and Eqs. (8-9) can not account for the states above the  $T = +\infty$  line. In fact, as proven in Refs. [28, 33], the grand canonical ensemble is not able to describe the localized phase  $h > 2a^2$ .

The microscopic evolution of the C2C model is implemented numerically with a microcanonical Monte Carlo (MMC) algorithm [34, 35]. According to this algorithm, random updates of the  $c_n$  are identified by the simplest moves that conserve mass and energy, simultaneously. Since two conservation laws imply two constraints we use a one-parameter evolution rule involving three sites, which we assume to be contiguous:  $(n-1, n, n+1)$ . In practice we pick up randomly a site  $n$  and we make a uniform choice of the new masses  $(c'_{n-1}, c'_n, c'_{n+1})$  such that: *i*) the total mass and total energy of the triplet are conserved and *ii*) the detailed balance is satisfied [34]. As explained in Appendix B this amounts to choose a random point in the intersection between a plane and a sphere, see the red dashed lines in Fig. 2. Because of the constraint  $c_n \geq 0$  such curve is either a circle or the union of three disjoint arcs, the latter case occurring when the mass of one of these sites is significantly larger than the other masses. Different arcs correspond to the same triplets where there has been a permutation of the sites such that the position of the peak has moved.

When the intersection of plane and sphere is given by three disjoint arcs we have two possible choices for the dynamics: either the new triplet of masses is forced to belong to the same arc containing the initial state or it is allowed to stay in any of the three arcs. In the former “pinned” case, high energy peaks cannot move to the neighboring sites, while in the latter case breathers can freely diffuse in the lattice (“unpinned” case). These two different update rules are equivalent in equilibrium

conditions [34] but they become inequivalent out of equilibrium.

When the C2C chain is attached to external reservoirs as in Fig. 2, the evolution proceeds by choosing a random site  $n = 1, \dots, N$  and distinguishing between inner ( $n = 2, \dots, N-1$ ) and outer ( $n = 1, N$ ) sites. For inner sites the triplet  $(n-1, n, n+1)$  belongs to the chain and evolution proceeds as for the MMC algorithm. For outer sites we perform a standard grand canonical Monte Carlo move according to given thermodynamic parameters  $X_L \equiv (\beta_L, \mu_L)$  (left boundary) and  $X_R \equiv (\beta_R, \mu_R)$  (right boundary). The details of reservoir dynamics are discussed in Appendix B. The rate of exchange of mass and energy from the reservoirs to the system can be measured by means of suitable definitions of mass- and energy fluxes. For the left boundary, we define

$$j_a^{(L)} = \frac{1}{\tau} \sum_{t_k=1}^{\tau} \delta c_1(t_k)$$

$$j_h^{(L)} = \frac{1}{\tau} \sum_{t_k=1}^{\tau} \delta c_1^2(t_k) \quad \tau \gg 1, \quad (10)$$

where  $\delta c_1(t_k)$  and  $\delta c_1^2(t_k)$  represent respectively the variations of mass and energy on the first lattice site produced by a Monte Carlo move of the reservoir occurring at time  $t_k$ . The definitions of  $j_a^{(R)}$  and  $j_h^{(R)}$  on the right boundary are readily obtained by replacing  $L \rightarrow R$  and  $c_1 \rightarrow c_N$  in Eq. (10)

When the external heat baths impose the same thermodynamic parameters at the chain ends,  $X_L = X_R$ , the system reaches thermodynamic equilibrium and  $j_a^{(L,R)} = j_h^{(L,R)} = 0$ . In this condition, mass- and energy densities fluctuate with respect to average values  $\bar{c}$  and  $\bar{c}^2$ , respectively. If heat baths work properly, we expect that  $\bar{c} = a$  and  $\bar{c}^2 = h$ , where  $a$  and  $h$  are related to the imposed values  $(\beta, \mu)$  through Eqs. (8-9). In Fig. 3 we show that this is indeed the case. In detail, isothermal ( $T = \text{const.}$ , left panel) and isochemical ( $\mu = \text{const.}$ , right panel) lines are here reproduced in the phase diagram  $(a, h)$ . A very good correspondence is found between numerical simulations and analytic predictions.

### III. LOCALIZATION IN OUT-OF-EQUILIBRIUM CONDITIONS

In this Section we study the C2C model in out-of-equilibrium conditions ( $X_L \neq X_R$ ) and discuss the emergence of localization. The left heat bath (attached to the site  $n = 1$ ) is defined by parameters  $\mu_L = 1$  and  $T_L = 0.1$ , which correspond to an average mass  $a_1 = 0.48$  and an average energy  $h_1 = 0.28$ . The right heat bath (attached to the site  $n = N$ ) is defined by  $\mu_R = 5$  and  $T_R = 5$ , which correspond to an average mass  $a_N = 2.69$  and an average energy  $h_N = 9.22$ . As anticipated, both boundary conditions are subcritical, i.e.  $h_1 < 2a_1^2$  and

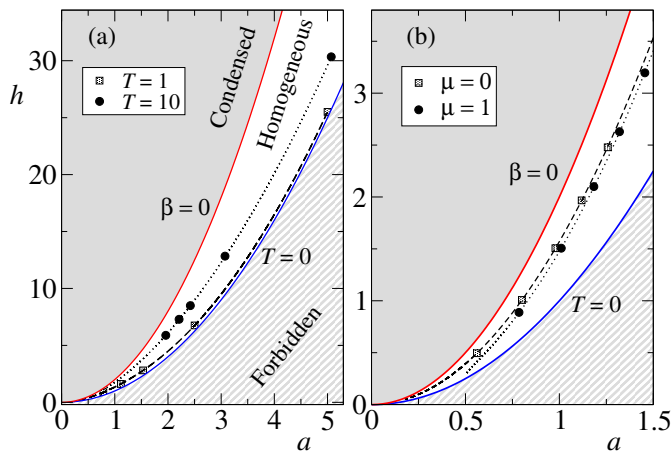


FIG. 3. Equilibrium phase diagram  $(a, h)$ : red and blue solid lines identify the critical line  $\beta = 0$  and the ground state  $T = 0$ , respectively. Heat baths are defined in the homogeneous region and are consistent with the grand canonical description of Eqs. (8-9). Here we compare the values of  $a$  and  $h$  obtained from grand canonical equilibrium simulations (full symbols) with the analytical curves relating  $(a, h)$  to  $(\beta, \mu)$  (continuous lines). Panels (a) and (b) show isothermals ( $T = \text{const}$ ) and isochemical ( $\mu = \text{const}$ ) lines, respectively.

$h_N < 2a_N^2$ . In Figs. 4 and 5 we highlight their position in the phase diagram with filled black circles. Initial conditions of the C2C chain are always chosen to be homogeneous and to connect the boundary values of  $a_1$  and  $a_N$ .

After a sufficiently long relaxation time  $\tau_0 \gtrsim 10^7$ , we perform a time average of the instantaneous mass and energy on each lattice site,

$$a_n = \frac{1}{\tau} \int_{\tau_0}^{\tau_0 + \tau} c_n(t) dt \quad (11)$$

$$h_n = \frac{1}{\tau} \int_{\tau_0}^{\tau_0 + \tau} c_n^2(t) dt \quad (12)$$

obtaining the corresponding time-average spatial profiles,  $a_n$  and  $h_n$ . If we plot  $h_n(a_n)$  we obtain a parametric curve in the space  $(a, h)$  which connects the circles corresponding to the thermal boundary conditions. In Fig. 4 we report our results for pinned dynamics (localized peaks can not diffuse in the lattice) while in Fig. 5 we show the results for the unpinned case (peaks freely diffuse). The main result is that in both cases the parametric curve enters the localization region  $h > 2a^2$  and a condensate is spontaneously created. Nevertheless, the condensation scenarios arising from these two dynamical rules are completely different.

### A. Dynamics with pinning

When pinning is imposed, a typical localized parametric profile is reported in the  $(a, h)$  plane in the main panel

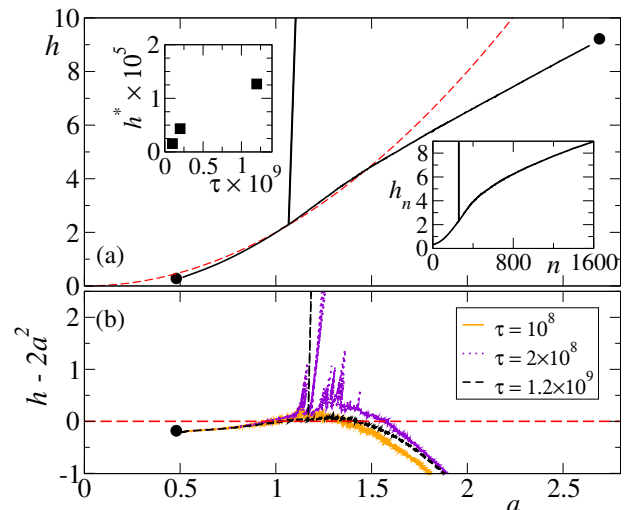


FIG. 4. Pinned dynamics. The red dashed lines correspond to the critical line  $h = 2a^2$ . (a) Parametric profile in the  $(a, h)$  plane for  $N = 1600$  and simulation time  $\tau = 1.2 \times 10^9$ . In the bottom right inset we plot the corresponding spatial energy profile  $h_n$ . Top left inset reports the peak's energy  $h^*$  as a function of time. (b) Parametric profiles for  $N = 12800$  at different times (see legend). The vertical axis reports the quantity  $h - 2a^2$ .

of Fig. 4(a) for  $N = 1600$  and a large simulation time  $\tau = 1.2 \times 10^9$ . The large peak close to the critical line  $h = 2a^2$  corresponds to a condensate localized on a single lattice site. The related energy density profile  $h_n$  is reported in the lower inset and shows that the nonlocalized portion of the chain gives rise to a smooth curve. In the presence of pinning, a large condensate localized on a lattice site cannot effectively jump on neighboring ones [34]. This property is found to hinder the relaxation to a nonequilibrium steady state, as the condensate absorbs a fraction of the energy flux transported through the chain (the effect on the mass flux is negligible because the mass is not condensed, energy is). As a result, the peak's energy  $h^*$  increases in time, as shown in the upper inset of Fig. 4(a) and boundary fluxes are unbalanced, i.e.  $j_a^{(L)} \neq -j_a^{(R)}$  and  $j_h^{(L)} \neq -j_h^{(R)}$ . The resulting nonequilibrium process is therefore non stationary. The spontaneous localization process is found to be stable against size variation: in Fig. 4(b) we show the parametric profiles for a larger chain ( $N = 12800$ ) at different simulation times. For more clarity, we plot on the vertical axis the quantity  $h - 2a^2$ : in this representation the critical line  $h = 2a^2$  maps to a horizontal line passing from the origin. Condensation starts when a smooth profile approaches and crosses the critical line, see solid orange curve. At intermediate times, the profile enters the localized region and a few localized states arise (dotted purple line). Finally, at larger times, a single condensed site remains (black short-dashed line), similarly to the case  $N = 1600$  shown in Fig. 4(a).

## B. Dynamics without pinning

When pinning is removed, localized energy can diffuse much more efficiently in the system and peaks can even attain the regions of the chain that are close to the reservoirs, i.e. in the homogeneous phase. This process has two important consequences. Firstly, it introduces an effective dissipation mechanism for condensed energy, which prevents the unlimited growth of the condensate, thereby allowing to attain a nonequilibrium stationary state at long times. This can be checked by comparing the incoming and outgoing fluxes of mass and energy. For the two transported quantities we have separately verified that in the long time limit  $(|j^{(L)}| - |j^{(R)}|)/(|j^{(L)}| + |j^{(R)}|) \rightarrow 0$ , as expected for stationary states. Secondly, peaks' diffusion smooths the density profiles and makes them linear, both in the parametric representation  $h(a)$  (see Fig. 5, main) and when plotted versus space (lower inset).

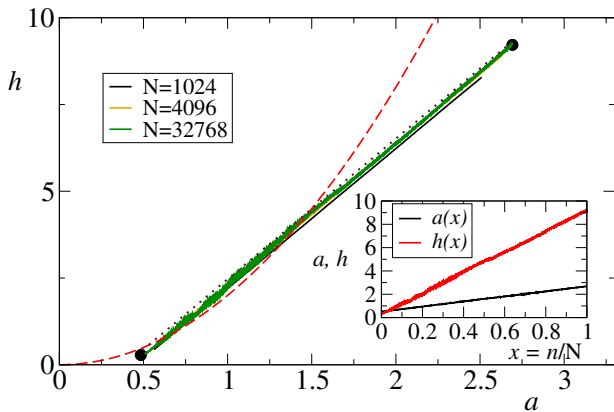


FIG. 5. Unpinned dynamics. Parametric profiles of the unpinned C2C model for the same boundary parameters as in Fig 4 and different system sizes. The dotted purple line is a reference straight line. The red dashed line is the critical line,  $h = 2a^2$ . Inset: spatial mass and energy profiles for the largest size  $N = 32768$ . For the largest size the stationary state was sampled for a time  $\tau = 2 \times 10^8$  units.

The nature of the dissipation mechanism and of the stationary state can be further clarified by monitoring the evolution of the instantaneous position and energy of the condensate, as shown in Fig 6. Panel (a) shows that the condensate position  $n^*(t)$  (black line), identified here as the lattice site with the highest energy in the whole chain, is approximately confined in the supercritical region  $h > 2a^2$ , between the two red dashed lines. We interpret this confinement as the evidence that the condensate can not survive too close to the reservoirs. Indeed the behavior of the condensate energy  $h^*(t)$  (panel (b)) confirms that when the condensate approaches the homogeneous region (specifically the side of the hotter reservoir) it undergoes a decay process that eventually destroys it. Remarkably, after this event a new condensate is created, in agreement

with the stationary nature of the process. The sequence of growth and decay cycles is found to depend on the system size: larger  $N$  produce slower cycles, with larger peaks (see different curves in panel (b)).

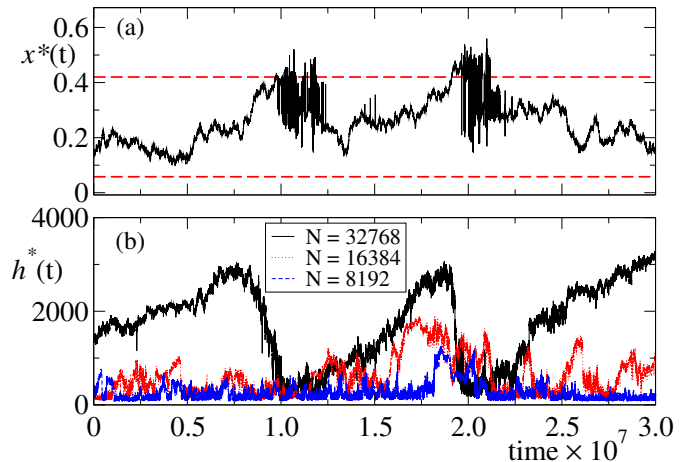


FIG. 6. Unpinned dynamics. Evolution of the condensate position  $x^*(t) \equiv n^*(t)/N$  for the largest size  $N = 32768$  and after the transient  $\tau_0$ . The two horizontal dashed lines identify the two positions where the stationary profile in (a) crosses the transition line  $h = 2a^2$ . For each time,  $n^*(t)$  is measured as the position of the site with largest energy along the chain. (c) Evolution of the condensate energy  $h^*(t) = \epsilon_{n^*(t)}$  on the same time scale of panel (b) and for different sizes.

Finally, in Fig. 7 we report the behavior of the mass ( $j_a$ ) and energy ( $j_h$ ) currents as a function of the system size  $N$  (we can now omit superscripts  $(L)$  and  $(R)$  because in a steady state left and right currents are equal). We find the standard scaling  $j_{a,h} \sim 1/N$ , which corresponds to normal, diffusive transport [36].

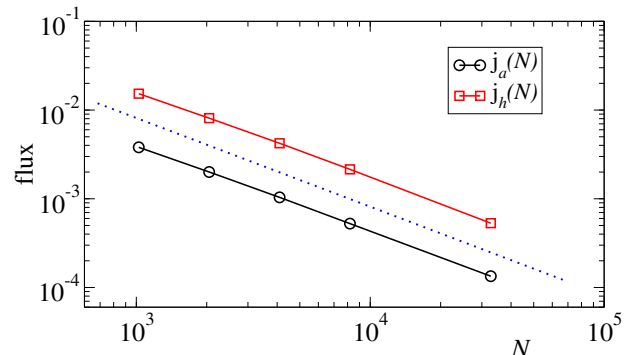


FIG. 7. Unpinned dynamics. Scaling of the stationary mass and energy fluxes *vs*  $N$ : the blue dotted line represents a diffusive scaling law  $j \sim N^{-1}$ .

#### IV. DISCUSSION

The observation of condensation phenomena in equilibrium conditions requires that the control parameter of the system exceeds a certain critical threshold. Such a condition has been realized in an isolated system initialized in the condensed region of parameters or imposing an overcritical boundary condition. In this paper, we have given evidence that a new mechanism is able to produce condensation when *i*) the system is kept out of equilibrium by boundary imbalances and *ii*) at least two independent quantities are transported (coupled transport). If taken individually, each boundary condition corresponds to a thermal state at finite temperature and belongs to the homogeneous, delocalized region. In fact, using standard heat baths like the Monte Carlo ones implemented here it would be impossible to equilibrate the system in the localized region [28]: localization emerges here because it is a pure nonequilibrium effect! The main question is therefore the role of the out-of-equilibrium setup in favoring the condensation process.

To clarify this point we propose a simple argument based on the dynamical evolution of a triplet of sites whose central site hosts a peak with large mass  $b$ . The two external sites of the triplet are supposed to be characterized by given mass distributions, imposed by the left and right reservoirs. Given this simplified picture, we analyze if on average the dynamical move favors the relaxation of the peak or on the contrary it may favor its growth. Let us therefore consider the triplet of masses  $(c_1, b, c_2)$  which evolves microcanonically towards  $(c_1 + x, b + \delta b, c_2 + y)$  in such a way that mass and energy are conserved,

$$x + y + \delta b = 0 \quad (13)$$

$$x^2 + y^2 + (\delta b)^2 + 2(c_1 x + c_2 y + b \delta b) = 0. \quad (14)$$

In equilibrium conditions  $c_1$  and  $c_2$  are drawn from the same distribution because boundary conditions are symmetric. In general it is convenient to write  $c_i = \bar{c}_i + \delta_i$ , where  $\bar{c}_i$  are the average values of the mass distributions at the left ( $i = 1$ ) and at the right ( $i = 2$ ) of the breather. From Eqs. (13-14) simple algebra allows to find the exact relation

$$\delta b(b - c) = -Q - (\delta_1 x + \delta_2 y) + \Delta(y - x), \quad (15)$$

where  $Q = \frac{1}{2}[x^2 + y^2 + (x + y)^2] \geq 0$  while  $c$  and  $\Delta$  are defined by the relations  $\bar{c}_1 = c + \Delta$  and  $\bar{c}_2 = c - \Delta$ . A value  $\Delta \neq 0$  means that we are out-of-equilibrium. Assuming  $b > c$  because  $b$  is a peak, a negative (positive) right-hand side of Eq. (15) means that the condensate decreases (increases) its mass. The first term on the right-hand side is negative-definite and it is at the origin of the condensate relaxation to equilibrium, because the second term fluctuates around zero ( $\bar{\delta}_i = 0$  by definition) and the third term vanishes for symmetric boundary conditions.

In out-of-equilibrium conditions,  $\Delta \neq 0$ , one finds that the transport of mass between the side with the largest  $\bar{c}_i$

and the opposite side determines that  $(y - x)$  has on average the same sign as  $\Delta$ . Therefore the out-of-equilibrium setup contributes to the variation of mass of  $b$  with a term which on average is positive. This clarifies that boundary imbalances favors the development of condensation.

We may now wonder about the relevance of having two conservation laws, especially in light of the results of Refs. [28, 33] where it is shown that the equilibrium properties of C2C model are equivalent to a model where only one quantity is conserved, the energy  $H = \sum_i \epsilon_i$ , but where  $\epsilon_i \geq 0$  are independent variables following the distribution  $f_\lambda(\epsilon) = (\lambda/2\sqrt{\epsilon}) \exp(-\lambda\sqrt{\epsilon})$ . For this model the critical value of the energy density  $h = H/N$  above which condensation appears is  $h_c = \langle \epsilon \rangle = 2/\lambda^2$  [37, 38]. If we attach such a lattice model to reservoirs at different temperatures, only a single current (the heat flux) can flow, and the resulting temperature profile must be monotonic [39]. Therefore, if boundary conditions are subcritical, i.e. they do not favor localization, the same must be true throughout the system. The above scenario is further confirmed by the study of the Zero-Range Process with open, asymmetric boundary conditions [21]. This is a model with only one conservation law and authors find localization only if boundary conditions allow it at equilibrium. It is also worth mentioning that in such case the condensate appears in proximity of the overcritical boundary.

#### V. PERSPECTIVES

As a future perspective of this work, coupled transport phenomenology of the C2C model will be worthy of complementary analysis from the point of view of linear response theory [40]. The main open questions include how the Onsager transport coefficients vary in the parameter space  $(a, h)$  and, in particular, whether they display any peculiar behavior when parametric curves cross the critical line  $h = 2a^2$ . It will also be interesting to understand in more detail how energy peaks are born and die in the unpinned case. In fact, these processes appear to be relevant both for the appearance of a nonequilibrium stationary state and of the linearity of mass and energy profiles, see the inset in Fig. 5.

In light of the importance of conservation laws it will be useful to study the observed condensation process in other models with conserved quantities. Among them, the DNLS equation is undoubtedly a relevant model to investigate. In fact, a closely related phenomenology was found in [41] when a DNLS chain was attached to a mass dissipator to one boundary and to a reservoir at the opposite boundary. A mass dissipator is not a proper reservoir, as it drives the system towards the point  $(a, h) = (0, 0)$ , which is singular thermodynamically, because any isothermal curve, including  $T = 0$  and  $T = \infty$ , terminates there, see Fig. 3(a). We also remark that despite the DNLS and C2C models display very similar equilibrium, critical properties, they have extremely



different relaxation dynamics [27, 42]: the frozen dynamics of localized states is a hallmark of the Hamiltonian dynamics of the DNLS equation and makes practically impossible to attain equilibrium in the condensed region. Therefore, the behavior of the DNLS model in the out-of-equilibrium setup studied here is an open question.

It would also be interesting to study other stochastic models where the local energy is not quadratic with the mass. In practice they are defined as a generalization of the C2C model where  $A = \sum_i c_i$  is unchanged and  $H = \sum_i c_i^\alpha$ . These models have been proposed in Ref. [31] and they are known to display condensation at equilibrium [30]. Their relaxation dynamics and nonequilibrium properties are not known.

More generally it would be useful to find suitable protocols for driving a system from the homogeneous to the localized phase. This would be relevant in some experimental contexts where the preparation of a system in the condensed region might be difficult because of dynamic or thermodynamic reasons [43].

## ACKNOWLEDGMENTS

Authors thank Antonio Politi for discussions and Federico Corberi for a critical reading of a first draft of the manuscript. PP acknowledges support from the MIUR PRIN 2017 project 201798CZLJ.

## Appendix A: The C2C model in the grand canonical ensemble

In this Appendix we derive explicitly the equilibrium properties of the C2C model within the grand canonical ensemble.

Given the two conserved quantities  $A$  and  $H$  in Eq. (4), the grand canonical partition function is

$$\begin{aligned} Z(\beta, \mu) &= \int_0^\infty dc_1 \dots dc_N e^{-\beta(H-\mu A)} \\ &= \int_0^\infty dc_1 \dots dc_N e^{-\beta(\sum_n c_n^2 - \mu \sum_n c_n)} \\ &= \prod_{n=1}^N \int_0^\infty dc_n e^{-\beta(c_n^2 - \mu c_n)} \\ &\equiv Z_0^N(\beta, \mu) \end{aligned} \quad (\text{A1})$$

where

$$Z_0(\beta, \mu) = \frac{1}{2} \sqrt{\frac{\pi}{\beta}} e^{\beta\mu^2/4} \left[ 1 + \operatorname{erf} \left( \frac{\sqrt{\beta}\mu}{2} \right) \right]. \quad (\text{A2})$$

The mass density  $a$  and the energy density  $h$  can be found from the equations

$$a = \frac{\langle A \rangle}{N} = \frac{1}{\beta} \frac{\partial}{\partial \mu} \ln Z_0 \quad (\text{A3})$$

$$h = \frac{\langle H \rangle}{N} = -\frac{\partial}{\partial \beta} \ln Z_0 + \mu a \quad (\text{A4})$$

which give Eqs. (8,9).

The curve corresponding to a vanishing temperature is easily found. In fact, for  $\beta \rightarrow +\infty$  Eq. (8) gives  $a = \mu/2$  and Eq. (9) gives  $h = a\mu/2 = a^2$ . The region  $h < a^2$  is not allowed as clearly shown by the evaluation of the variance of the mass distribution,

$$\sigma^2 \equiv \bar{c}^2 - (\bar{c})^2 = h - a^2 \geq 0. \quad (\text{A5})$$

The curve corresponding to a diverging temperature ( $\beta \rightarrow 0$ ) is more subtle because the first term on the right-hand side of Eq. (9) diverges. In the same limit Eq. (8) would give an unphysical diverging mass if  $\mu$  keeps finite. It is therefore necessary that  $\mu$  diverges as well and the correct divergence is such that  $\beta\mu = -\gamma$ , where  $\gamma$  is a finite, positive constant. Expanding the erf function in Eq. (8) we find

$$a \simeq -\frac{1}{\beta\mu} + \frac{4}{\beta^2\mu^3} \quad (\text{A6})$$

and Eq. (9) finally gives

$$h = \frac{2}{\beta^2\mu^2} = 2a^2. \quad (\text{A7})$$

## Appendix B: Dynamics of the C2C model

A Monte Carlo time step is composed by a sequence of  $N$  attempted moves, where  $N$  is the number of sites. An attempted move starts choosing a random site  $k = 1, \dots, N$ . If  $k = 1$  or  $k = N$  we implement the heat baths as explained here below. If  $k \neq 1, N$  we consider the triplet of consecutive sites  $(k-1, k, k+1)$  and we perform a microcanonical move of the masses  $(c_{k-1}, c_k, c_{k+1})$ , i.e. a transition towards a new triplet  $(c'_{k-1}, c'_k, c'_{k+1})$  having the same mass and energy,

$$c_{k-1} + c_k + c_{k+1} = M = c'_{k-1} + c'_k + c'_{k+1} \quad (\text{B1})$$

$$c_{k-1}^2 + c_k^2 + c_{k+1}^2 = E = (c'_{k-1})^2 + (c'_k)^2 + (c'_{k+1})^2 \quad (\text{B2})$$

and chosen uniformly in the solution space of previous equations.

In practice, Eqs. (B1-B2) define the intersection between a plane and a sphere, with the constraint that all new masses are positive (see Fig. 2). This intersection (which is non-zero because there is the solution  $c'_i = c_i$ ,  $i = k-1, k, k+1$ ) is either a circle (if all  $c_i$  are of the same order) or the sum of three disjoint arcs of a circle (if one  $c_i$  is much larger than the other two). Solutions can be parameterized by an angle whose random choice ensures that detailed balance is locally satisfied.

We have implemented Monte Carlo heat baths attached to the lattice sites  $k = 1$  and  $k = N$  as follows. Once that one of the two external sites is randomly chosen we perform an attempt of variation of its mass,

$$c_k \rightarrow c'_k = c_k + \psi, \quad (\text{B3})$$

where  $\psi$  is a random variable uniformly distributed in the interval  $(-\psi_k, \psi_k)$ . If  $c'_k \geq 0$  we accept the move

according to the Metropolis rule with the cost function

$$W = e^{-(\Delta H - \mu_k \Delta A)/T_k}, \quad (\text{B4})$$

where  $(T_k, \mu_k)$  are the temperatures and the chemical potentials of the heat baths,  $\Delta H = (c_k + \psi)^2 - c_k^2$ , and  $\Delta A = \psi$ . We have tested several values of  $\psi_1$  and  $\psi_N$  and we generally used  $\psi_1 = \psi_N = 0.5$ .

- 
- [1] S. N. Majumdar, S. Krishnamurthy, and M. Barma, Nonequilibrium phase transitions in models of aggregation, adsorption, and dissociation, *Physical review letters* **81**, 3691 (1998).
- [2] J. Eggers, Sand as maxwell's demon, *Physical Review Letters* **83**, 5322 (1999).
- [3] G. M. Schütz, Critical phenomena and universal dynamics in one-dimensional driven diffusive systems with two species of particles, *Journal of Physics A: Mathematical and General* **36**, R339 (2003).
- [4] Y. Kafri, E. Levine, D. Mukamel, G. M. Schütz, and J. Török, Criterion for phase separation in one-dimensional driven systems, *Physical review letters* **89**, 035702 (2002).
- [5] C. Godrèche, Dynamics of condensation in zero-range processes, *Journal of Physics A: Mathematical and General* **36**, 6313 (2003).
- [6] M. R. Evans and T. Hanney, Nonequilibrium statistical mechanics of the zero-range process and related models, *Journal of Physics A: Mathematical and General* **38**, R195 (2005).
- [7] S. Majumdar, Real-space condensation in stochastic mass transport models, *Exact Methods in Low-dimensional Statistical Physics and Quantum Computing: Lecture Notes of the Les Houches Summer School: Volume 89, July 2008*, 407 (2010).
- [8] J. Török, Analytic study of clustering in shaken granular material using zero-range processes, *Physica A: Statistical Mechanics and its Applications* **355**, 374 (2005).
- [9] M. Zannetti, F. Corberi, and G. Gonnella, Condensation of fluctuations in and out of equilibrium, *Physical Review E* **90**, 012143 (2014).
- [10] R. Pastor-Satorras and C. Castellano, Distinct types of eigenvector localization in networks, *Scientific reports* **6**, 1 (2016).
- [11] H. Eisenberg, Y. Silberberg, R. Morandotti, A. Boyd, and J. Aitchison, Discrete spatial optical solitons in waveguide arrays, *Physical Review Letters* **81**, 3383 (1998).
- [12] F. Lederer, G. I. Stegeman, D. N. Christodoulides, G. Asanto, M. Segev, and Y. Silberberg, Discrete solitons in optics, *Physics Reports* **463**, 1 (2008).
- [13] J.-M. Drouffe, C. Godrèche, and F. Camia, A simple stochastic model for the dynamics of condensation, *Journal of Physics A: Mathematical and General* **31**, L19 (1998).
- [14] S. N. Majumdar, M. Evans, and R. Zia, Nature of the condensate in mass transport models, *Physical review letters* **94**, 180601 (2005).
- [15] C. Godrèche, From urn models to zero-range processes: statics and dynamics, in *Ageing and the glass transition* (Springer, 2007) pp. 261–294.
- [16] C. Godrèche, Condensation and extremes for a fluctuating number of independent random variables, *Journal of Statistical Physics* **182**, 1 (2021).
- [17] G. Gotti, S. Iubini, and P. Politi, Finite-size localization scenarios in condensation transitions, *Physical Review E* **103**, 052133 (2021).
- [18] C. Godrèche and J.-M. Luck, Condensation in the inhomogeneous zero-range process: an interplay between interaction and diffusion disorder, *Journal of Statistical Mechanics: Theory and Experiment* **2012**, P12013 (2012).
- [19] J. Barré and L. Mangeolle, Condensation with two constraints and disorder, *Journal of Statistical Mechanics: Theory and Experiment* **2018**, 043211 (2018).
- [20] T. Kriecherbauer and J. Krug, A pedestrian's view on interacting particle systems, kpz universality and random matrices, *Journal of Physics A: Mathematical and Theoretical* **43**, 403001 (2010).
- [21] E. Levine, D. Mukamel, and G. Schütz, Zero-range process with open boundaries, *Journal of statistical physics* **120**, 759 (2005).
- [22] P. G. Kevrekidis, *The discrete nonlinear Schrödinger equation: mathematical analysis, numerical computations and physical perspectives*, Vol. 232 (Springer Science & Business Media, 2009).
- [23] K. Rasmussen, T. Cretegny, P. G. Kevrekidis, and N. Grønbech-Jensen, Statistical mechanics of a discrete nonlinear system, *Physical review letters* **84**, 3740 (2000).
- [24] S. Iubini, S. Lepri, and A. Politi, Nonequilibrium discrete nonlinear schrödinger equation, *Physical Review E* **86**, 011108 (2012).
- [25] S. Iubini, S. Lepri, R. Livi, and A. Politi, Coupled transport in rotor models, *New Journal of Physics* **18**, 083023 (2016).
- [26] S. Iubini, R. Franzosi, R. Livi, G.-L. Oppo, and A. Politi, Discrete breathers and negative-temperature states, *New Journal of Physics* **15**, 023032 (2013).
- [27] A. Politi, P. Politi, and S. Iubini, Frozen dynamics of a breather induced by an adiabatic invariant, *Journal of Statistical Mechanics: Theory and Experiment* **2022**, 043206 (2022).
- [28] G. Gradenigo, S. Iubini, R. Livi, and S. N. Majumdar, Localization transition in the discrete nonlinear schrödinger equation: ensembles inequivalence and negative temperatures, *Journal of Statistical Mechanics: Theory and Experiment* **2021**, 023201 (2021).
- [29] T. Mithun, Y. Kati, C. Danieli, and S. Flach, Weakly nonergodic dynamics in the gross-pitaevskii lattice, *Physical review letters* **120**, 184101 (2018).
- [30] F. Mori, G. Gradenigo, and S. N. Majumdar, First-order condensation transition in the position distribution of



- a run-and-tumble particle in one dimension, *Journal of Statistical Mechanics: Theory and Experiment* **2021**, 103208 (2021).
- [31] J. Szavits-Nossan, M. R. Evans, and S. N. Majumdar, Constraint-driven condensation in large fluctuations of linear statistics, *Physical review letters* **112**, 020602 (2014).
- [32] J. Szavits-Nossan, M. R. Evans, and S. N. Majumdar, Condensation transition in joint large deviations of linear statistics, *Journal of Physics A: Mathematical and Theoretical* **47**, 455004 (2014).
- [33] G. Gradenigo, S. Iubini, R. Livi, and S. N. Majumdar, Condensation transition and ensemble inequivalence in the discrete nonlinear schrödinger equation, *The European Physical Journal E* **44**, 1 (2021).
- [34] S. Iubini, A. Politi, and P. Politi, Coarsening dynamics in a simplified dnls model, *Journal of Statistical Physics* **154**, 1057 (2014).
- [35] S. Iubini, A. Politi, and P. Politi, Relaxation and coarsening of weakly-interacting breathers in a simplified dnls chain, *Journal of Statistical Mechanics: Theory and Experiment* **2017**, 073201 (2017).
- [36] S. Lepri, R. Livi, and A. Politi, Thermal conduction in classical low-dimensional lattices, *Physics reports* **377**, 1 (2003).
- [37] C. Godrèche and J. Luck, Nonequilibrium dynamics of the zeta urn model, *The European Physical Journal B-Condensed Matter and Complex Systems* **23**, 473 (2001).
- [38] M. Evans, S. N. Majumdar, and R. Zia, Canonical analysis of condensation in factorised steady states, *Journal of Statistical Physics* **123**, 357 (2006).
- [39] S. Lepri, *Thermal transport in low dimensions: from statistical physics to nanoscale heat transfer*, Vol. 921 (Springer, Heidelberg, 2016).
- [40] R. Livi and P. Politi, *Nonequilibrium statistical physics: a modern perspective* (Cambridge University Press, 2017).
- [41] S. Iubini, S. Lepri, R. Livi, G.-L. Oppo, and A. Politi, A chain, a bath, a sink, and a wall, *Entropy* **19**, 445 (2017).
- [42] S. Iubini, L. Chirondojan, G.-L. Oppo, A. Politi, and P. Politi, Dynamical freezing of relaxation to equilibrium, *Physical review letters* **122**, 084102 (2019).
- [43] M. Baldovin, S. Iubini, R. Livi, and A. Vulpiani, Statistical mechanics of systems with negative temperature, *Physics Reports* **923**, 1 (2021).